Korean J. Chem. Eng., 35(2), 594-601 (2018)
DOI: 10.1007/s11814-017-0304-x

pISSN: 0256-1115
eISSN: 1975-7220

Physicochemical analysis of linear low-density polyethylene composite films containing chemically treated rice husk

Ki Seob Hwang*, Hyuk Jun Kwon, and Jun-Young Lee*,†**

*Korea Institute of Industrial Technology, 89 Yangdaegiro-gil, Ipjang-myeon, Seobuk-gu, Cheonan-si, Chungcheongnam-do 31056, Korea
**Department of Chemical Engineering, Yonsei University, 134 Shinchon-dong, Seodaemoon-gu, Seoul 03722, Korea
(*Received 25 February 2017 • accepted 5 November 2017*)

Abstract−A study was conducted to determine the appropriate surface treatment for rice husks (RH) in polymer composite film to improve the physical properties relative to those of untreated RH/linear low-density polyethylene (LLDPE) film. Pulverized RH was treated with NaOH (RH-m) and acetic acid (RH-ac) to prepare composite films with LLDPE resin. The treated RH showed typical mercerization and acetylation, as confirmed by spectroscopic and thermal analysis methods. The RH-m sample was mercerized, allowing decomposition of hemicellulose and partially amorphous cellulose. The RH-ac sample was processed via acetylation inducing partial lignin decomposition. Field-emission scanning electron microscopy showed smaller gaps at the RH/LLDPE interface for RH-m and RH-ac compared to that with untreated RH, implying increased composite compatibility. RH-m in particular showed superior tensile strength (15.85 N/mm^2), elongation (884%), Young's modulus (60.01 N/mm^2), and tear strength (7.71 N/mm^2) compared to untreated RH and RH-ac.

Keywords: Rice Husks, Physicochemical Analysis, Rice Husk/LLDPE Composite Film, Mercerizing, Acetylation

INTRODUCTION

Polyethylene (PE) is used in many applications, including packaging comprising flexible films produced by the blown film process. Significant differences in physical properties are observed in low-density PE (LDPE), linear low-density PE (LLDPE), and high-density PE (HDPE) blown films. HDPE is the most crystalline PE, with linear chains containing very little branching. It shows a high modulus, intermediate tensile properties, and poor tear resistance. LDPE, containing long-chain branches on the order of 1-3 per 1000 carbon atoms, as well as 10-30 short-chain branches per 1000 carbon atoms, shows a low tensile strength and modulus and intermediate tear resistance. LLDPE has a wide range of short-chain branching and generally good tensile and tear resistance. The type and amount of short-chain branching significantly affect the physical properties [1].

LLDPE is an important commercial polymer widely used for different applications in modern technology. It has a higher tensile strength and tear resistance than LDPE and is very flexible with good elongation under stress; LLDPE can make thinner films with better resistance to environmental stress cracking [2].

LLDPE films are extensively used for the packaging industry, foodstuffs, goods packaging, agriculture, and merchandizing [3,4]. Food packaging is the fastest-growing sector in the packaging market [5,6], and packaging industry consumes more than 40% of the plastics with half of it for food packaging [7,8]. However, the use of petroleum-based polymers generates a significant amount of greenhouse gases and depletes natural resources, while contaminating the planet with toxic byproducts during polymer decomposition. Moreover, the cost of petroleum-based polymers is relatively higher than that of other agricultural byproduct materials.

To improve the mechanical strength and reduce the use of fossil fuel-based plastics, many producers use polymer composites with various filler materials. Rice husk (RH) is an agricultural byproduct produced during the milling process; 70 million of tons of RH are generated in china annually [9], with 150 million tons produced globally in 2012 [10]. However, many researchers [11-14] have considered utilizing RH-based biomass as a composite material for petroleum-based plastics, which could eventually reduce the production of petroleum-based plastic materials. Compared to inorganic fillers such as carbon black, calcium carbonate, talc, and zinc oxide, RHs are lighter, more economical, and provide higher strength per weight [15].

In general, RH consists of silica (20 wt%) as a silicon-cellulose membrane [16], cellulose (35-45 wt%), hemicellulose (19-25 wt%), lignin (20 wt%), and wax (14-17 wt%) [10,12,17,18]. Recent studies of polymer- and biomass-based natural composites showed promising results for many different applications such as bio-degradable polymers [19-21], reinforcing fillers [22-24], building materials [25], and merchandise packaging [4-8]. The mercerization of the RH in these composites induces increased hydrophilicity, predominantly from the large increase in bands associated with hydroxyl groups, and increased crystallinity from the reduction of amorphous structures. The mercerization of RH using alkali treatment with sodium hydroxide (NaOH) has been used to improve the RH-matrix interfacial bonding. NaOH removes natural fats and

†To whom correspondence should be addressed.
E-mail: jaylee@kitech.re.kr

waxes from the cellulose fiber surfaces, revealing chemically reactive functional groups such as hydroxyls. The acetylation of RH is also used to modify the surface of RH, inducing greater hydrophobicity. "Acetylation" describes the introduction of an acetyl functional group to an organic compound. The acetylation of RH coats the RH surface hydroxyl groups, which are responsible for hydrophilicity, with hydrophobic molecules [12,26-32].

We investigated the characteristics of modified rice husk-polymer composite film for merchandise packaging with improved physical properties. We prepared LLDPE composite films with RHs surface-treated with either aqueous NaOH solution or acetic acid. These treated RH/LLDPE composite films were evaluated with physical and chemical analysis to determine their applicability as food packaging films with mechanical properties approaching those of LLDPE films.

EXPERIMENTAL

1. Materials

The RHs were obtained from PyeongTaek, SongTan, and milled with an air classifying mill (ACM, AU, Inc.) to particle form. Particle analysis with a particle size distribution meter showed RH particles of 0.32-79.62 μm with a mean size of 6.3 μm (hereafter, RH refers to untreated rice husks). For RH surface treatment, NaOH (Samchun Chemical, 98% purity) and acetic acid (AA, Sigma-Aldrich, ACS reagent, ≥99.7% purity) were used as reagents. Deionized water (DI water, Dream Plus II, JEIO-TECH) was used as a solvent. Finally, LLDPE (melt index value ASTM D1238 1.2 g/10 min, Lotte Chemical, UL 912A grade) resin was used to produce the composites. To facilitate compounding between LLDPE and RH with and without surface treatments, Zn-stearate (Sinwon Chemicals) and polyethylene wax (PE-wax, Korea Petrochemical) were employed.

2. RH Surface Treatment Using NaOH or Acetic Acid

NaOH-treated RH (RH-m) was prepared via the following treatment procedure. 6 g NaOH was dissolved in 200 mL DI water and stirred for 30 min. Then, 20 g RH was added to the NaOH aqueous solution and stirred for 30 min at room temperature to mercerize. Next, the RH in aqueous NaOH was centrifuged for 5 min at 6,000 rpm and washed with DI water; the washing procedure was repeated three times to reach neutral pH. After the mercerizing treatment in NaOH aqueous solution, RH-m was prepared by drying the washed RH in a dry oven at 80 °C for 24 h. The preparation of RH-m was performed three time, and their characteristics were not different.

The preparation of AA-treated RH (RH-ac) was similar to that of RH-m. 6 g AA was dissolved in 200 mL DI water and stirred for 30 min. Then, 20 g RH was added and stirred for 30 min at room temperature to acetylate in aqueous AA. RH was filtered from the AA solution using filter paper and a Buchner funnel, and then washed with running DI water for 15 min. After surface acetylation treatment in the AA solution, RH-ac was prepared by drying the washed RH in a dry oven at 80 °C for 24 h. The preparation of RH-ac was performed three time, and their characteristics were not different.

RH-m and RH-ac were pulverized using a ball mill and sieved with 74 mesh before further analysi.

3. Film Formation via Extrusion and Blowing

RH, RH-m, and RH-ac were each employed as 10% by weight of the total film composition; the balance was LLDPE. Specifically, 14 g each of RH, RH-m, and RH-ac was used with 126 g of LLDPE for each film type. An activator and resin stabilizer of 4 g of PE-wax and 1 g of Zn-stearate, respectively, were added.

The RH, RH-m, or RH-ac, LLDPE, and additives were added to a high-speed mixer (SHR-10A high-speed mixer, Nanjing Xiu Lin Machinery Manufacturer Co., Ltd.). Mixing was performed until the internal temperature reached 80 °C, followed by extrusion with a small twin extruder (XL20 Twin-screw Extruder Machine, Nanjing Xiu Lin Machinery Manufacturer Co. Ltd.) with the length-to-diameter ratio of 32 : 1 and a 55-mm screw diameter. For temperature control, the chamber was set with eight heating zones of different temperatures (130, 140, 150, 160, 170, 180, 190, and 190 °C at the hopper, six heating chambers, and die, respectively), while operating at the average spin rate of 800 rpm. The extruded materials were cooled to room temperature using an air fan. The obtained compound was sliced into 3-4-mm slices using a cutting machine for pelletization.

Film formation involved using a single extrusion of 30 mm (length/diameter=7 : 1) to inject the compound into the film blowing machine (SMC film blowing machine, Zhangjigang City Lianjiang Machinery Co. Ltd.). Each sample was prepared separately. The four heating zones were set to 200, 180, 180, and 150 °C. The produced film had a thickness of 120±3 μm.

4. Characterization of Modified RH and RH/LLDPE Films

A thermogravimetric analyzer (TGA-50, SHIMADZU) was used for materials characterization. In the analysis, 10 mg each of RH, RH-m, and RH-ac were heated from 30 °C to 600 °C at a rate of 10 °C/min under a high-purity nitrogen atmosphere (N_2 99.99%, 50 mL/min) to prevent unwanted oxidation processes.

X-ray diffractometry (XRD) experiments for the RH, RH-m, and RH-ac samples were conducted using a D8 ADVANCE (Bruker AXS GmbH, Germany). The diffraction patterns were obtained at room temperature with a monochromatic Cu Kα radiation source (λ=0.1542 nm) in stepping mode with a 2θ angle range from 5° to 90° with a step size of 0.03° and scanning time of 5.0 min.

X-ray photoelectron spectroscopy (XPS) analysis of RH, RH-m, and RH-ac was conducted using an ESCA 2000 (Thermo Scientific). The analysis area was 600 μm^2, with the energy of 0-3 kV and radiation of Mg Kα (0.7 eV) and Al Kα (0.85 eV). The samples were mounted on a holder using double-sided tape. A pressure of 10^{-8} Pa was used with 1.0 eV energy and the pass energy of 21 eV was employed for survey scanning.

^{13}C cross-polarization/magic-angle spinning nuclear magnetic resonance (CP/MAS ^{13}C NMR) spectroscopy measurements were performed with a Bruker 400 MHz solid-state FT-NMR spectrometer equipped with a solid-state high-resolution apparatus. The operating frequency of ^{13}C is 100.62 MHz. The conventional CP/MAS method was used for the high-resolution solid-state ^{13}C NMR measurements. The rotors containing the RH samples were spun at 12 kHz with the 90° pulse, contact time, and repetition time of 4 μs, 2 ms, and 3 s, respectively. For each spectrum, 4096 scans were recorded. The ^{13}C chemical shifts were calibrated through the car-

bonyl C resonance of glycine at 176.03 ppm as an external reference and converted to the values from tetramethylsilane (TMS). The nonlinear least-squares method was used for line fitting with the Lorentzian function previously described [33].

Fourier-transform infrared (FT-IR) spectroscopic analysis was performed using the transmittance method in the range of 4,000-400 cm^{-1}. Here, 1% of each sample (RH, RH-m, or RH-ac) was pelletized using KBr powder, and the spectra were obtained after 20 scans with the resolution of 4 cm^{-1}.

RH and RH/LLDPE, RH-m/LLDPE, and RH-ac/LLDPE composite films were frozen by immersion in liquid nitrogen and crushed before being coated with gold. The surface information and morphologies of the gold-coated samples were obtained using a JEOL JSM-6701F scanning electron microscope (SEM).

RH/LLDPE, RH-m/LLDPE, and RH-ac/LLDPE composite films were analyzed according to ASTM D882 to measure the tensile strength, elongation, and Young's modulus, and according to ASTM D1938-67 to measure the tear strength. Each sample was submitted to the QM 100SE quality measurement system (QMESYS Inc.) and tested with a 50-mm/min crosshead speed and 20-N load cell. The mechanical properties evaluations were repeated five times for each film type to obtain the average values.

RESULTS AND DISCUSSION

To determine the thermal stability of RH, RH-m, and RH-ac, TGA was conducted, as shown in Fig. 1. The RH samples show mass losses in three different stages (stage I: 32-140 °C; stage II: 141-378 °C; stage III: 379-480 °C) with 29% of the mass remaining after the experiment. The first stage corresponds to the gradual evaporation of absorbed moisture (because of the hydrophilic character of the lignocellulose) and the dehydration and degradation of hemicellulose [17,34]. After some stabilization time, in the second stage, decomposition of amorphous cellulose and partial

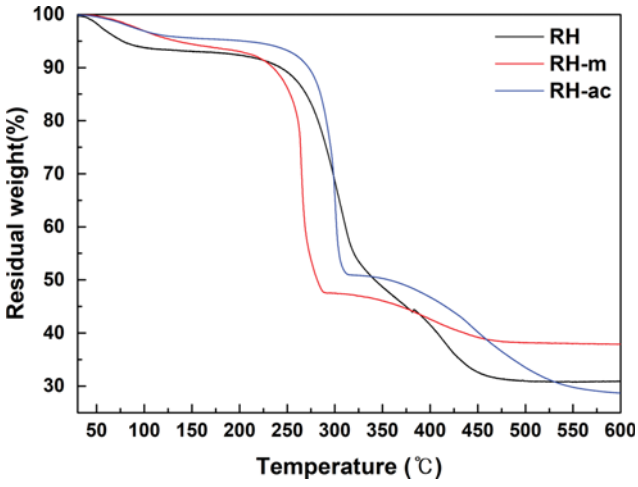

Fig. 1. Thermal stability of RH, RH-m, and RH-ac by TGA curves.

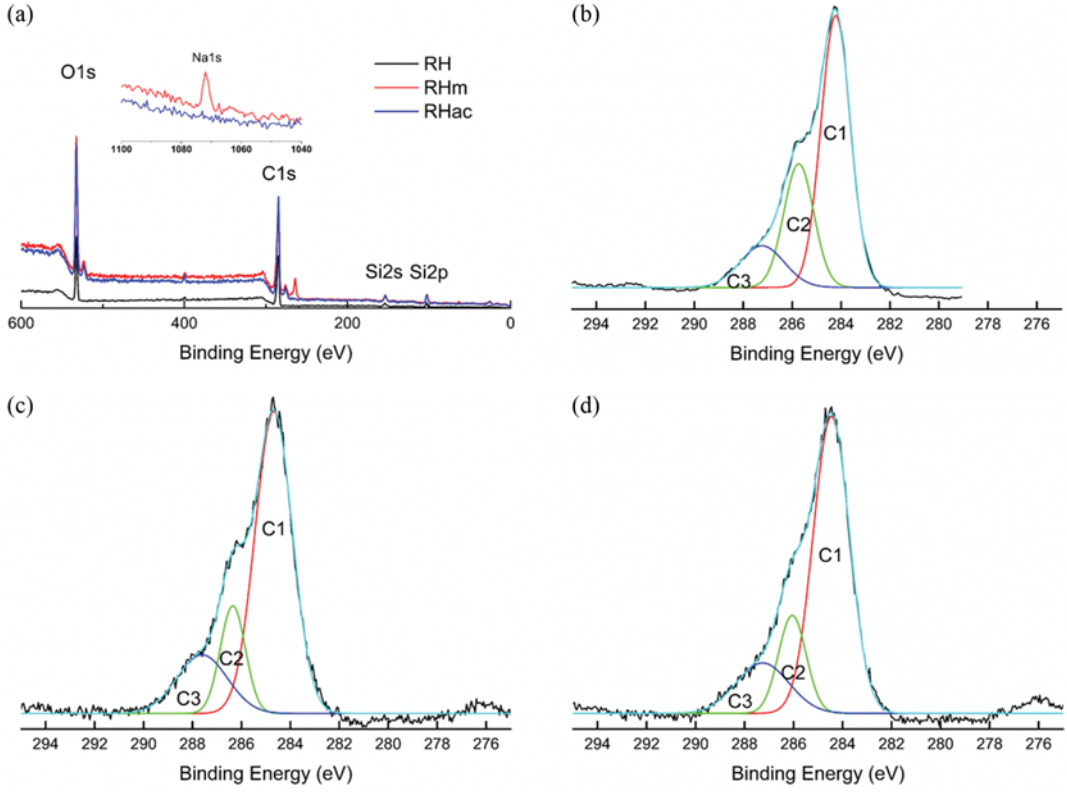

Fig. 2. X-ray photoelectron spectra for the observation of elemental composition and structural changes; (a) the general scan spectra of RH (without modification), RH-m (modified with NaOH), and RH-ac (modified with acetic acid), (b) C1s scan spectrum of RH, (c) C1s scan spectrum of RH-m, and (d) C1s scan spectrum of RH-ac.

hemicellulose occurs at 200 °C, and hemicellulose decomposes until 290 °C [17]. According to the literature, amorphous cellulose degradation is easier than that of crystalline cellulose and lignin [35]. In the third stage, the decomposition of the remaining cellulose, crystalline cellulose, and lignin is observed; decomposed and incompletely oxidized char [17] remain after the temperature of the final mass loss.

The TGA of RH-m also shows three stages (stage I: 34-166 °C, stage II: 167-289 °C, stage III: 290-478 °C), with 38% of the mass remaining after the experiment. Compared to RH, the end temperature of stage II occurs 89 °C lower in RH-m, while only a 2 °C difference is observed for stage III. As reported by Ndazi et al. [36], RH-m has lower thermal stability than RH. Moreover, RH-m is more susceptible to losses during stage II, indicating the partial decomposition of hemicellulose in alkali solution, which induces the termination of the second stage at a lower temperature [37]. The remaining mass difference is ascribed to the presence of sodium salts.

In the thermal mass loss curves of RH-ac compared to those of RH-m, stage I for both samples occurs at 34-150 °C, stage II of RH-ac occurs at 313 °C, and stage III occurs at 540 °C. The acetylation of RH increases the temperatures of stage II and III for RH-ac. In stage III, the decomposition of crystalline cellulose and lignin and the deacetylation of RH-ac occur simultaneously [38].

XPS analysis was conducted to confirm the elemental composition and structural changes of RH, RH-m, and RH-ac. As shown in Fig. 2(a), all samples contain carbon (C 1*s* at 284 eV), oxygen (O 1*s* at 532 eV), nitrogen (N 1*s* at 400 eV), and silicon (Si 2*s* at 152 eV, Si 2*p* at 103 eV) [39]. Because of hydrolysis, sodium ions (Na 1*s* at 1,070 eV) are observed only in the RH-m sample. The elemental analysis data is summarized in Table 1.

Compared to RH, RH-m shows lower carbon content and higher silicon content (Si 2*s* and Si 2*p*) from the decomposition of partial hemicellulose, with cellulose and lignin remaining major components [12]. The mercerization process removes natural fats, waxes, lignin, and hemicellulose from the RH surface, according to Eq. (1). The removal of these surface impurities also improves the surface roughness of both cellulose fibers and particles.

$$\text{Cellulose}-\text{OH}+\text{NaOH}\rightarrow\text{Cellulose}-\text{ONa}+\text{H}_2\text{O}+\text{impurities} \quad (1)$$

Compared to RH, RH-ac shows less carbon and much more silicon. This result indicates that acetylation by AA decomposes the acid-soluble lignin [40]. The acid-soluble lignin in RH was extracted upon acetylation and removed during washing.

To confirm the above observations, the C 1*s* spectra were further analyzed to verify hybridization of the carbon centers. We observed C-C, C=C, and C-H peaks at (C 1, 284.6 eV), C-O and C-N at (C 2, 286.3 eV) [41,42], and O-C-O at (C 3, 287.6 eV) [43], as summarized in Fig. 2(b)-(d) for RH, RH-m, and RH-ac. In Fig. 2(b), the C 1*s* region of RH shows C1 content of 59.1%, C2 of 27.3%, and C3 of 13.6%.

Table 1. Elemental analysis with chemical treated rice husk by XPS

	C (%)	O (%)	N (%)	Si (%)	Na (%)
RH	68.5	25.4	1.74	4.32	0
RH-m	60.2	28.7	1.53	7.20	2.36
RH-ac	64.2	25.9	1.89	7.95	0

Table 2. C1s composition ratio with RH surface treatment through XPS analysis. Three replicate spectra are shown from three spots on the sample

	C1 (%)	C2 (%)	C3 (%)
RH	59.1	27.3	13.6
RH-m	66.5	16.0	17.5
RH-ac	66.8	16.8	16.4

Compared to RH, the carbon content of RH-m has a C1 content of 66.5%, C2 of 16.0%, and C3 of 17.5%, as shown in Fig. 2(c). This indicates fewer C-O bonds and more C-C bonds from the decomposition of hemicellulose by NaOH. Fig. 2(d) shows C1 content of 66.7%, C2 of 16.8%, and C3 of 16.4% for RH-ac, similar to the results obtained for RH-m. As mentioned, these results are attributed to lignin decomposition by acetic acid.

As shown in Table 2, the C 1*s* composition ratios for RH, RH-m, and RH-ac are confirmed through XPS analysis. RH comprises amorphous and crystalline cellulose, hemicellulose, lignin, and silica. To verify changes in crystallinity before and after surface treatment, XRD analysis is performed. Fig. 3 shows the XRD results for RH, RH-m, and RH-ac. All samples show a broad diffuse peak at $2\theta=22^{\circ}$, indicating an amorphous structure. The peak at $2\theta=23.7^{\circ}$ is known to arise from partially crystalline cellulose [44]. Compared to the other samples, RH-m shows relatively sharp peaks because NaOH removes natural fats, waxes, silica, lignin, and hemicellulose [45]. So, compared to the pattern of RH, the peak of RH-m at $2\theta=22^{\circ}$ with amorphous structure is decreased because the amorphous structure of cellulose I begins regenerating and swelling in concentrated alkali [46]. Moreover, RH-m shows additional peaks at 25.7°, 35.3°, and 38.0°, among others, indicating recrystallization [47-49] after NaOH hydrolysis.

To analyze the molecular structures of RH, RH-m, and RH-ac,

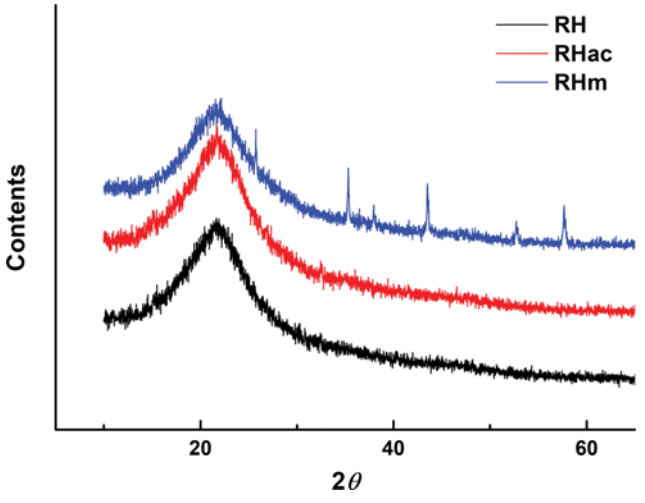

Fig. 3. XRD analysis results for RH (without modification), RH-m (modified with NaOH), and RH-ac (modified with acetic acid).

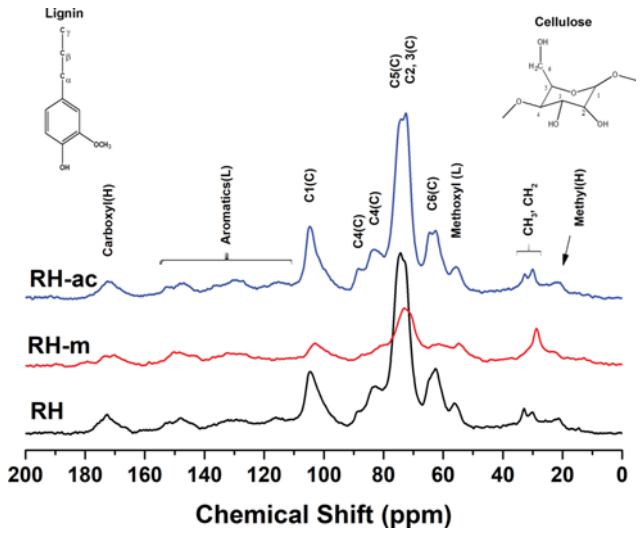

Fig. 4. Molecular structure analysis of RH (without modification), RH-m (modified with NaOH), and RH-ac (modified with acetic acid) analyzed by ^{13}C CP/MAS NMR.

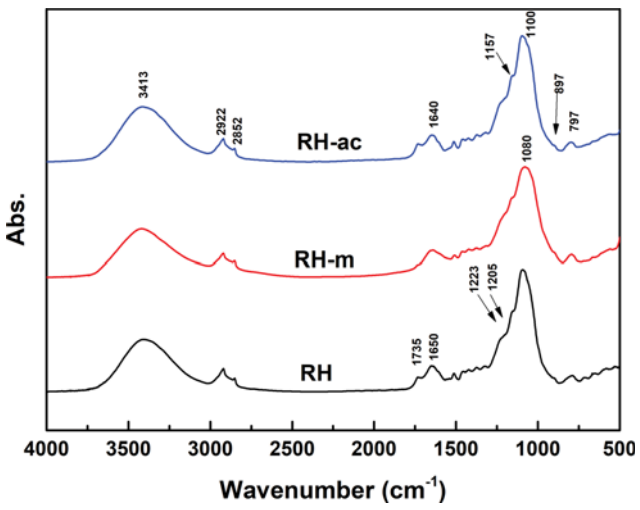

Fig. 5. FT-IR spectra for RH (without modification), RH-m (modified with NaOH), and RH-ac (modified with acetic acid) showing the functional group changes after RH surface treatment modification.

^{13}C CP/MAS NMR analysis was conducted, with spectra shown in Fig. 4. The structures of cellulose, hemicellulose, and lignin, the main components of RH, are indicated. Carbon atoms of carbohydrates are generally in the 50-100 ppm range. The peak at 21 ppm corresponds to the methyl carbon of the hemicellulose acetyl groups; this does not appear in the spectrum of RH-m because most hemicellulose is decomposed by NaOH. Carboxylic carbon atoms of hemicellulose appear at 175 ppm [50,51]. Carbon atoms of cellulose appear with C1 at 105 ppm, C4 of crystalline cellulose at 89 ppm, C4 of amorphous cellulose at 84 ppm, C5 at 75 ppm, C2 and C3 at 73 ppm, and C6 at 64 ppm. The carbon atoms of lignin are shown in the methoxyl group at 57 ppm and in aromatic carbons at 115-150 ppm. Further carbon atoms of lignin appear at 31 ppm and 33 ppm.

Compared to RH, RH-m shows a significant difference in the carbon structure of cellulose. A significant decrease of the C4 and C6 peaks is observed from mercerization by NaOH, which reduces the hydrogen bonding of α-crystalline cellulose and partially interferes with the crystalline structure [26]. In addition, RH-ac shows a shift of the C6 signal from 62 to 64 ppm, which can be explained by the reaction of cellulose with hydroxide [52]. This produces an increase in added methoxyl groups on cellulose (hydroxyl parts) via acetylation and coupling reactions; thus, compared to RH, we observe a decreased C5 and increased C2 and C3.

To detect functional group changes in RH-m and RH-ac compared to RH, FT-IR is used to analyze RH, RH-m, and RH-ac, as shown in Fig. 5. The FT-IR spectrum of RH shows the O-H stretching vibration of cellulose at 3,413 cm^{-1}, O-H stretching vibrations of intermolecular hydrogen bonds in cellulose at ~3,300 cm^{-1} (overlapping in the ~3,600-3,250 cm^{-1} range), and asymmetric and symmetric C-H stretching in CH_3 and CH_2 at 2,922 and 2,852 cm^{-1} in cellulose and lignin, respectively. Additionally, the C=O stretching of carbonyl groups in lignin is shown at 1,735 cm^{-1}. Peaks at 1,223 cm^{-1}, 1,205 cm^{-1}, and 1,100 cm^{-1} indicate C-O-C and C-O(-H) stretching vibrations. Moreover, both symmetric (877 cm^{-1}) and asymmetric (797 cm^{-1}) Si-O stretching signals are observed [12,17, 19,32].

The RH-m sample shows a lower-intensity peak at 1,735 cm^{-1} compared to that for RH, indicating the decomposition and removal of carbonyl groups in lignin after alkali treatment. Moreover, the shoulder at 1,223 cm^{-1} is shifted to 1,205 cm^{-1} from reactions between silica bonds and NaOH. The decrease of the Si-O bond peak at 797 cm^{-1} is ascribed to the hydrolysis of silica bonds in alkali solution [12,36]. The RH-ac sample shows an increased peak at 1,735 cm^{-1} compared to that in RH, from the addition of acetyl groups to cellulose after the acetylation reaction with AA. Finally, the peak at 1,157 cm^{-1} is increased by the ester functionality of the acetyl group [38].

Fig. 6 shows the FE-SEM images of pulverized RH. For RH-m and RH-ac samples, FE-SEM analysis is conducted after compounding with LLDPE and processing the composite film.

RH shows rifted shapes of various diameters. Furthermore, the inside and outside of the RH are mixed during the pulverization process. Therefore, we employed the powders both before and after surface treatment in compounding with LLDPE to produce composite films and analyzed their morphologies. We confirmed the presence of surface gaps (in the circle) between LLDPE and RH from the composite film sample in Fig. 6(b)-(d). This affects the mechanical properties. For the RH-m/LLDPE composite film, the sample shows dense attachment between RH-m and LLDPE, indicating good compatibility for film formation. The obtained composite film with RH-ac shows features similar to the RH composite film with voids at the interface with LLDPE. However, we observe thread-shaped connective material at the RH-ac/LLDPE matrix interface. These could be from surface treatment by acetylation [53].

Figs. 7 and 8 show the mechanical properties of tensile strength, elongation (Fig. 7), Young's modulus, and tear strength (Fig. 8) of LLDPE and RH/LLDPE, RH-m/LLDPE, and RH-ac/LLDPE composite films. The tensile strength of LLDPE is 21.6±1.3 N/mm^2 on

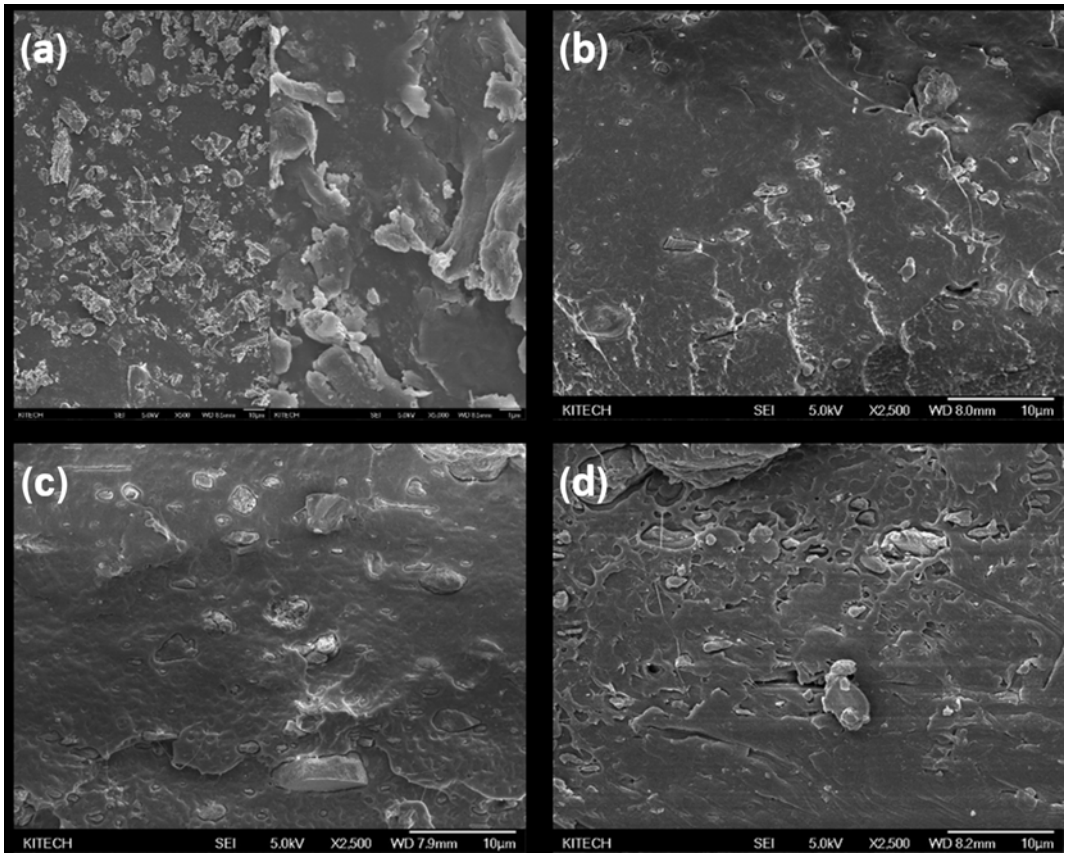

Fig. 6. FE-SEM images of films with LLDPE and treated RH. (a) is pulverized RH (without modification), (b) is RH/LLDPE composite film, (c) is RH-m/LLDPE composite film, and (d) is RH-ac/LLDPE composite film.

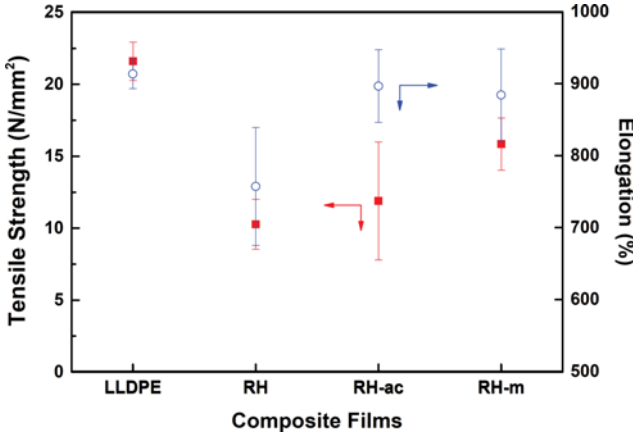

Fig. 7. Tensile strength and elongation of LLDPE and films using RH (without modification), RH-m (modified with NaOH), and RH-ac (modified with acetic acid).

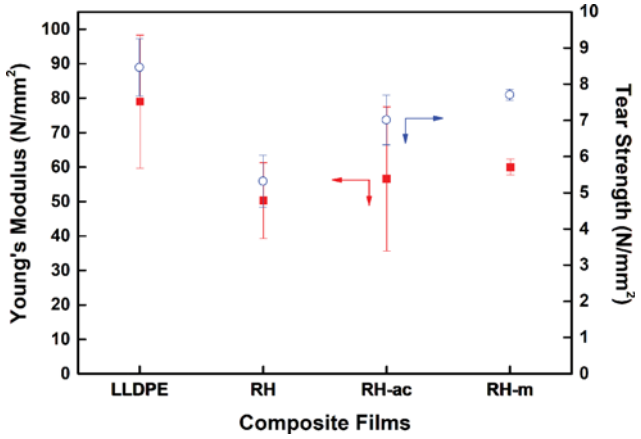

Fig. 8. Young's modulus and tear strength of LLDPE and films using RH (without modification), RH-m (modified with NaOH), and RH-ac (modified with acetic acid).

average with 913±20% elongation. Meanwhile, RH/LLDPE, RH-m/LLDPE, and RH-ac/LLDPE composite films showed tensile strengths of 10.27±1.74, 15.85±1.81, and 11.89±4.10 N/mm^2, respectively, and elongations of 757±82, 884±64, and 896±50%, respectively. Young's modulus and tear strength were 78.96±19.31 N/mm^2 and 8.47±0.79 N/mm^2 for LLDPE film, 50.26±11.00 N/mm^2 and 5.32±0.72 N/mm^2 for RH/LLDPE film, 60.01±2.33 N/mm^2 and 7.71±0.15 N/mm^2 for RH-m/LLDPE film, and 56.60±20.93 N/mm^2 and 7.01±0.69 N/mm^2 for RH-ac/LLDPE film, respectively.

In comparing these results, we conclude that the tensile strength, elongation, Young's modulus, and tear strength of the surface-treated samples are increased after NaOH treatment. Among the composites, the RH-m/LLDPE composite film shows remarkable improvement, which is explained by the relatively high crystallinity and low

carbonyl content according to XRD, XPS, and FT-IR analysis. Furthermore, fewer C=O bonds are detected in RH-m/LLDPE, creating a higher morphological density than that of the RH-ac/LLDPE composite film. Moreover, the RH-m/LLDPE composite film has higher tensile strength, Young's modulus, and tear strength than the RH/LLDPE and RH-ac/LLDPE composite films do because the RH-m swelled and recrystallized during mercerizing. The tear strength is an important property for films applied in packaging. The elongation of RH-m/LLDPE composite films is less than that of RH-ac/LLDPE composite films. For the RH-ac/LLDPE composite film, the compatibility is increased compared to RH/LLDPE composite film by the acetylation of cellulose. Nevertheless, gap formation at the interface between RH-ac and LLDPE induces the lowest tensile strength and elongation of the composite films.

CONCLUSIONS

We presented various surface treatment methods for RH as filler applied in film blowing processes. NaOH was employed for the mercerization of RH (RH-m), and acetic acid for the acetylation of the cellulose surface (RH-ac). In particular, RH-m showed partial decomposition of hemicellulose and amorphous cellulose, while maintaining lignin and crystalline structure as major components. During the composite film formation using the blowing method, both untreated and surface-treated RHs were well tolerated. The composite film produced using RH-m showed a dense structure without voids at the RH-m/LLDPE interface, as well as superior properties with a tensile strength, elongation, Young's modulus, and tear strength of 15.85 N/mm^2, 884%, 60.01 N/mm^2, and 7.71 N/mm^2, respectively. For films produced using RH filler, the present study confirmed that RH surface treatment process provides physical properties similar to those of LLDPE, allowing the production of RH/LLDPE composites. Through the chemical analysis of the LLDPE composite films with chemically treated RH, LLDPE composite films with eliminated or decreased hemicellulose and amorphous cellulose in RH were determined to be more compatible with higher physical properties relative to composites with untreated RH. According to the results of this study, RH-m and LLDPE composite film has similar physical properties to LLDPE film, so it is considered to be applicable for merchandise packaging.

ACKNOWLEDGEMENTS

This works supported by Korea Institute of Planning and Evaluation for Technology in Food, Agriculture, forestry (IPET) through High Value-added Food Technology Development Program, funded by Ministry of Agriculture, Food and Rural Affairs (MAFRA) (114008).

REFERENCES

1. X. M. Zhang, S. Elkoun, A. Ajji and M. A. Huneault, *Polymer.*, **45**, 217 (2004).
2. G. Chandran V and S. D. Waigaonkar, *Polymer Composites.*, **37**, 2995 (2016).
3. D. A. Pereira de Abreu, P. Paseiro Losada, I. Angulo and J. M. Cruz, *European Polymer J.*, **43**, 2229 (2007).
4. A. Dorigato and A. Pegoretti, *Engineering Fracture Mechanics.*, **79**, 213 (2012).
5. K. W. McMillin, *Meat Sci.*, **132**, 153 (2017).
6. N. Bumbudsanpharoke and S. Ko, *J. Food Sci.*, **80**, R910 (2015).
7. K. Majeed, A. Hassan, A. A. Bakar and M. Jawaid, *J. Thermoplast. Compos. Mater.*, **29**, 1003 (2014).
8. S. D. F. Mihindukulasuriya and L. T. Lim, *Trends Food Science Technol.*, **40**, 149 (2014).
9. S. J. Yoon, Y.-I. Son, Y.-K. Kim and J.-G. Lee, *Renewable Energy*, **42**, 163 (2012).
10. J. H. Kwon, N. Ayrilmis and T. H. Han. *Composites Part B: Engineering*, **44**, 728 (2013).
11. R. S. Chen, M. H. Ab Ghani, M. N. Salleh, S. Ahmad and M. a. A. Tarawneh, *J. Appl. Polymer Sci.*, **132** (2015), DOI:10.1002/app.41494.
12. S.-K. Yeh, C.-C. Hsieh, H.-C. Chang, C. C. C. Yen and Y.-C. Chang, *Composites Part A: Appl. Sci. Manufacturing*, **68**, 313 (2015).
13. N. Petchwattana, S. Covavisaruch and S. Chanakul, *J. Polymer Res.*, **19** (2012), DOI:10.1007/s10965-012-9921-6.
14. I. Ahmad, C. E. Lane, D. H. Mohd and I. Abdullah, *Composites Part B: Engineering*, **43**, 3069 (2012).
15. H.-S. Kim, H.-S. yang, H.-J. Kim and H.-J. Park, *J. Therm. Anal. Calorimetry*, **76**, 395 (2004).
16. S. F. Korablev and D. S. Korablev, *Powder Metall. Met. Ceram.*, **54**, 106 (2015).
17. N. Johar, I. Ahmad and A. Dufresne, *Industrial Crops and Products*, **37**, 93 (2012).
18. N. Soltani, A. Bahrami, M. I. Pech-Canul and L. A. González, *Chem. Eng. J.*, **264**, 899 (2015).
19. J. Mohammadi-Rovshandeh, P. Pouresmaeel-Selakjani, S. M. Davachi, B. Kaffashi, A. Hassani and A. Bahmeyi, *J. Appl. Polymer Sci.*, **131** (2014), DOI:10.1002/app.41095.
20. N. Johar and I. Ahmad, *BioResources.*, **7**, 5469 (2012).
21. M. K. Mohamad Haafiz, S. J. Eichhorn, A. Hassan and M. Jawaid, *Carbohydr. Polym.*, **93**, 628 (2013).
22. N. Ayrilmis and A. Kaymakci, *Industrial Crops and Products.*, **43**, 457 (2013).
23. K. Merkel, H. Rydarowski, J. Kazimierczak and A. Bloda, *Composites Part B: Engineering*, **67**, 138 (2014).
24. U. Buyuksari, N. Ayrilmis and T. Akbulut, *J. Appl. Polymer Sci.*, **123**, 1740 (2012).
25. D. B. Dittenber and H. V. S. GangaRao, *Composites Part A: Appl. Sci. Manufacturing*, **43**, 1419 (2012).
26. S. L. Fávaro, M. S. Lopes, A. G. Vieira de Carvalho Neto, R. Rogério de Santana and E. Radovanovic, *Composites Part A: Appl. Sci. Manufacturing*, **41**, 154 (2010).
27. W. A. W. A. Rahman, S. Lee Tin, A. R. Rahmat, N. M. Isa, M. S. N. Salleh and M. Mokhtar, *J. Compos. Mater.*, **45**, 1403 (2010).
28. A. Salanti, L. Zoia, M. Orlandi, F. Zanini and G. Elegir, *J. Agric. Food Chem.*, **58**, 10049 (2010).
29. M. Zurina, H. Ismail and A. A. Bakar, *J. Appl. Polymer Sci.*, **92**, 3320 (2004).
30. A. Bazargan, M. Bazargan and G. McKay, *Renewable Energy*, **77**, 512 (2015).
31. Y. Li, G. Li, Y. Zou, Q. Zhou and X. Lian, *Cellulose*, **21**, 301 (2013).
32. Z. Wang, J. P. Barford, C. W. Hui and G. McKay, *Chem. Eng. J.*,

281, 961 (2015).
33. H. Kono, C. Oka, R. Kishimoto and S. Fujita, *Carbohydr. Polym.*, **170**, 23 (2017).
34. S. M. L. Rosa, N. Rehman, M. I. G. de Miranda, S. M. B. Nachtigall and C. I. D. Bica, *Carbohydr. Polym.*, **87**, 1131 (2012).
35. P. W. M. Peters, J. Hemptenmacher and H. Schurmann, *Composites Sci. Technol.*, **70**, 1321 (2010).
36. B. S. Ndazi, S. Karlsson, J. V. Tesha and C. W. Nyahumwa, *Composites Part A: Appl. Sci. Manufacturing*, **38**, 925 (2007).
37. F. Fahma, S. Iwamoto, N. Hori, T. Iwata and A. Takemura, *Cellulose*, **18**, 443 (2010).
38. H. Salmah, F. Amri and H. Kamarudin, *Polymer-Plastics Technol. Eng.*, **51**, 86 (2012).
39. S. M. Morsi, A. Pakzad, A. Amin, R. S. Yassar and P. A. Heiden, *J. Colloid Interface Sci.*, **360**, 377 (2011).
40. M. Simon, Y. Brostaux, C. Vanderghem, B. Jourez, M. Paquot and A. Richel, *J. Chem. Technol. Biotechnol.*, **89**, 128 (2014).
41. E. Y. L. Teo, L. Muniandy, E.-P. Ng, F. Adam, A. R. Mohamed, R. Jose and K. F. Chong, *Electrochim. Acta*, **192**, 110 (2016).
42. J. Lu, P. Askeland and L. T. Drzal, *Polymer*, **49**, 1285 (2008).
43. A. Zarrouk, B. Hammouti, T. Lakhlifi, M. Traisnel, H. Vezin and F. Bentiss, *Corrosion Sci.*, **90**, 572 (2015).
44. S. D. Genieva, S. C. Turmanova, A. S. Dimitrova and L. T. Vlaev, *J. Therm. Anal. Calorimetry*, **93**, 387 (2008).
45. S. Chakraborty, S. Chowdhury and P. Das Saha, *Carbohydr. Polym.*, **86**, 1533 (2011).
46. Y. Liu and H. Hu, *Fibers and Polymers*, **9**, 735 (2008).
47. A. M. Das, A. A. Ali and M. P. Hazarika, *Carbohydr. Polym.*, **112**, 342 (2014).
48. P. Lu and Y.-L. Hsieh, *Carbohydr. Polym.*, **82**, 329 (2010).
49. A. Trubetskaya, P. A. Jensen, A. D. Jensen, M. Steibel, H. Spliethoff, P. Glarborg and F. H. Larsen, *Biomass Bioenergy*, **86**, 76 (2016).
50. J. C. C. Freitas, T. J. Bonagamba and F. G. Emmericha, *Carbon*, **39**, 535 (2001).
51. C. R. Teixeira Tarley, S. L. Costa Ferreira and M. A. Zezzi Arruda, *Microchem. J.*, **77**, 163 (2004).
52. K. Miura and T. Nakano, *Mater. Sci. Eng. C Mater. Biol. Appl.*, **53**, 189 (2015).
53. H. Yang, R. Yan, H. Chen, D. H. Lee and C. Zheng, *Fuel*, **86**, 1781 (2007).